

Experimental study and ab initio molecular orbital calculation on the photolysis of *n*-butyrophenone included within the alkali metal cation-exchanged ZSM-5 zeolite

Hiromi Yamashita^{a,*}, Shingo Takada^a, Masahiko Hada^b,
Hiroshi Nakatsuji^b, Masakazu Anpo^{a,*}

^a Department of Applied Chemistry, Graduate School of Engineering, Osaka Prefecture University, Gakuen-cho 1-1, Sakai, Osaka 599-8531, Japan

^b Department of Synthetic Chemistry and Biological Chemistry, Graduate School of Engineering, Kyoto University, Sakyo-ku, Kyoto 606-8501, Japan

Received 10 December 2002; received in revised form 15 January 2003; accepted 10 April 2003

Abstract

Effects of ion-exchanged alkali metal cations on the adsorption and the photolysis (Norrish type I and type II reactions) of *n*-butyrophenone included within the alkali metal cation-exchanged ZSM-5 zeolite have been investigated by experimental and theoretical approaches. The yields of the photolysis decreased and the ratio of the type I/type II reactions increased, respectively, by changing the ion-exchanged cations from Cs⁺ to Li⁺. The observed IR spectra of the adsorbed *n*-butyrophenone and the ab initio molecular orbital calculations of this host–guest system indicate that the *n*-butyrophenone mainly interacts with alkali metal cation, while the electrostatic interaction between the *n*-butyrophenone and cation increases by changing the cations from Cs⁺ to Li⁺. These results indicate that the smaller cation has the stronger electrostatic interaction between *n*-butyrophenone and promotes the Norrish type I reaction in the photolysis of *n*-butyrophenone. © 2003 Elsevier Science B.V. All rights reserved.

Keywords: Photolysis; Zeolite; Alkali metal cation; Butyrophenone; Molecular orbital calculation; Electrostatic interaction

1. Introduction

Investigations on the photophysics and photochemistry of molecules adsorbed on solid surfaces such as SiO₂ and zeolites have attracted a great deal of attention in heterogeneous photochemistry and/or surface photochemistry. One of the most interesting aims in this field is to determine what the influences are to the photophysical and photochemical properties of the adsorbed molecules when the micro-environment of the adsorption sites is modified and changed in its physical and/or chemical nature. It is well known that the photophysical and photochemical behavior of adsorbed molecules are quite different from those observed in gas and liquid phases. Zeolites are considered to be one of the most suitable materials in investigating a variety of host–guest interactions and their role in the photochemical nature of the guest molecules [1–16]. Since the pioneering works of Turro and Ramamurthy et al. [12–16], studies of the photophysics and photochemistry of molecules

included within the restricted cavities of zeolites have been the focus of many studies relating to the effects of the micro-environment. Charge-compensating cations are exchangeable and bring about variations in the physical characteristics of the micro-environment of the adsorption sites of zeolites [1–16]. It has been reported that the presence of light-atom cations such as Li⁺ and Na⁺ can modify the photochemical behavior of the guest molecules through their high positive charge density and electrostatic potentials [12–16].

In the present study, the effects of ion-exchanged alkali metal cations on the adsorption state and the photochemical properties of *n*-butyrophenone included within the zeolite cavities have been investigated at the molecular level by spectroscopic measurements, ab initio molecular orbital calculations as well as analysis of the photolysis of ketone molecules.

2. Experimental details

ZSM-5 zeolites (Si/Al ratio = 11) calcinated at 773 K for 7 h were used as adsorbents. Alkali metal cation-exchanged

* Corresponding author.

E-mail address: yamashita@chem.osakafu-u.ac.jp (H. Yamashita).

¹ Co-corresponding author. Tel./fax: +81-72-254-9287.

zeolites were prepared by an ion-exchange method using the nitrate aqueous solution of the cation. The ion-exchanged percentages of these cations on ZSM-5 were determined by atomic absorption spectroscopy: 83% for Li^+ ; 83% for Na^+ ; 82% for K^+ ; and 75% for Cs^+ , respectively. Adsorption of *n*-butyrophenone from the gas phase into the zeolite cavities was carried out using a conventional vacuum system after the evacuation of the zeolite samples to 10^{-6} Torr at 295 K. The amount of *n*-butyrophenone introduced into the samples was about 1.2×10^{-5} mol/g. This value corresponds to the ratio of added ketones and ion-exchanged cations (Li^+); $\sim 1\%$. IR measurements were carried out at 295 K using a JASCO FT-IR 7600 [5]. The desorption temperatures of the pre-adsorbed *n*-butyrophenone on various cation-exchanged zeolites were determined from IR measurements carried out after the evacuation of the samples at various temperatures. Photolysis of the *n*-butyrophenone was carried out at 273 K using a high pressure mercury lamp ($\lambda > 270$ nm) in a quartz cell (50 cm^3) connected to a closed evacuation system. The reaction products in the gas phase which were trapped after evacuation, such as propane, propylene, ethylene were analyzed by gas chromatography. The ab initio molecular orbital calculations for the interaction between the ketones and alkali metal cations were performed using a Gaussian 98 package. The equilibrium geometries and harmonic vibrational frequencies were computed at HF(SCF) levels. The geometry of the zeolite framework model used in the present study was obtained by the optimization of the geometry of the model representing the $\text{T}_{12}\text{-O}_{24}\text{-T}_{12}\text{-O}_7\text{-T}_3$ site of ZSM-5 which is a part of the framework at the cross-section with the straight channel and the sinusoidal channel of the ZSM-5 zeolite [17–19]. The basis sets were: the 6-31G* type for H,

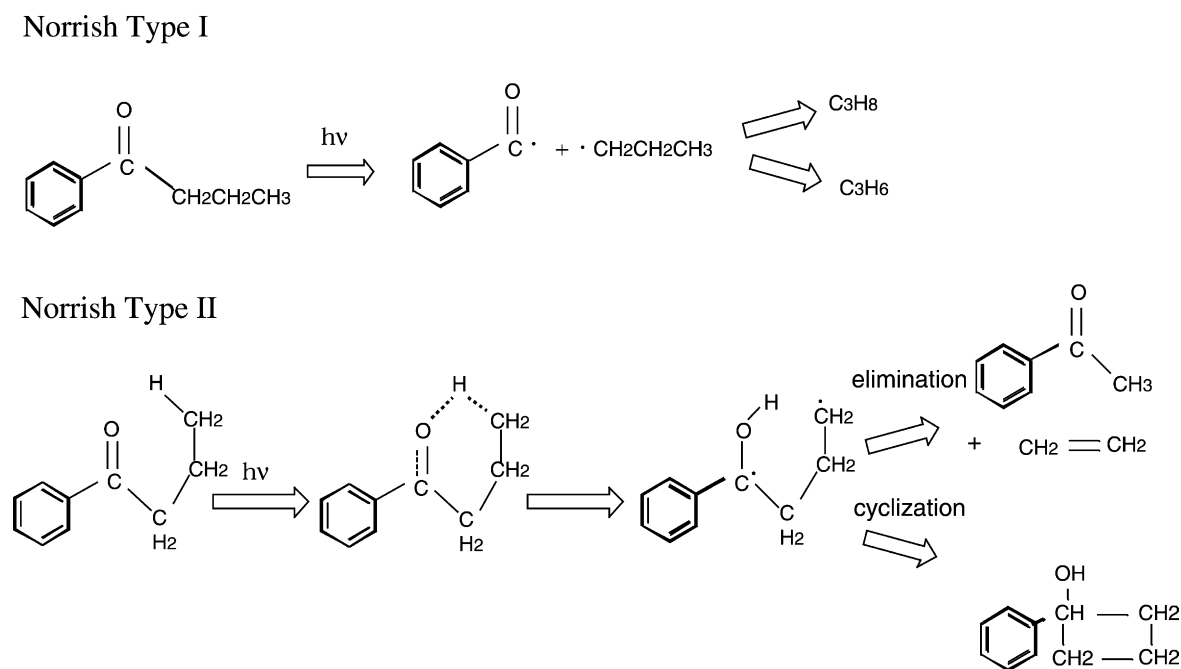
C, O of the ketone; (8s6p)/[3s3p] for K, Rb, Cs; and 6-31G for H, Si, Al, O, Li, Na of the zeolite framework and the alkali metal. Wadt-Hay ECP was added to K, Rb, Cs [9].

3. Results and discussion

3.1. Photolysis of *n*-butyrophenone and spectroscopic measurements for the *n*-butyrophenone–zeolite interactions

n-Butyrophenone having γ -hydrogen atoms undergoes the Norrish type I process (α -cleavage into radical pairs) and the Norrish type II process (intramolecular elimination) as shown in Scheme 1 [6,20,21]. It is also known that the only Norrish type II reaction including such cyclization processes proceeds in the gas phase reaction. Propane and propylene are formed either by a hydrogen atom abstraction by a propyl radical or a hydrogen atom elimination from a propyl radical formed in the Norrish type I cleavage, respectively. Ethylene and acetophenone are formed in the Norrish type II reaction. Therefore, the yields of the Norrish type I and type II reactions can be determined from the yields of these products.

Table 1 shows the effect of the kind of cations on the photolysis of *n*-butyrophenone included within the alkali metal cation-exchanged ZSM-5 zeolites. In the photolysis of *n*-butyrophenone included within the zeolite cavities, the major products were ethylene and acetophenone from the Norrish type II reaction, while the products from Norrish type I reaction, propylene and propane, are also observed. The reaction selectivity of Norrish type I (type I/(type I + type II)) in the photolysis of *n*-butyrophenone are 9–0.08,



Scheme 1. Mechanism of the photolysis of *n*-butyrophenone.

Table 1
The yields of products in the photolysis of *n*-butyrophenone included within alkali metal cation-exchanged ZSM-5 zeolites^a

Cations	Yields of products ^b ($\times 10^{-7}$ mol/g)	Type I ^c selectivity (%)	A/B ^d (%)
H ⁺	0.01	20	
Li ⁺	0.07	9	0.01
Na ⁺	1.3	0.3	0.1
K ⁺	3.2	0.2	8
Rb ⁺	3.5	0.1	29
Cs ⁺	0.01	0.06	61
SiO ₂ (Aerosil 380)	10.7	0.08	

^a Photolysis condition: $\lambda > 270$ nm, 273 K, 2 h.

^b The total amount of products in type I (C₂H₄) and type II (C₃H₆ + C₃H₈).

^c The type I selectivity is the ratio of yields; type I/(type I + type II).

^d A: total amount of products in type I (C₂H₄) and type II (C₃H₆ + C₃H₈). B: intensity of IR band of adsorbed *n*-butyrophenone.

being much larger than those obtained for the corresponding photolysis in the gas phase where the only products from Norrish type II were observed. In the cavities of the ZSM-5 zeolite, the Norrish type I reaction is promoted considerably [13–16]. As shown in Table 1 the total yields decrease and the ratios of the Norrish type I/type II increase with changing the cations from Cs⁺ to Li⁺. Because the change in the yields of Norrish type I are very small ($0.1\text{--}0.6 \times 10^{-9}$ mol/g), the change in the yields of Norrish type II with the change of cations reflected significantly on the changes in the total yields and the reaction ratios. These results clearly indicate that the photolysis of *n*-butyrophenone included within the zeolite cavities is strongly affected by the change in the chemical nature of the micro-environment of the adsorption sites by exchanging the cations.

Fig. 1 shows the IR spectra of *n*-butyrophenone included within the alkali metal cation-exchanged ZSM-5 zeolite

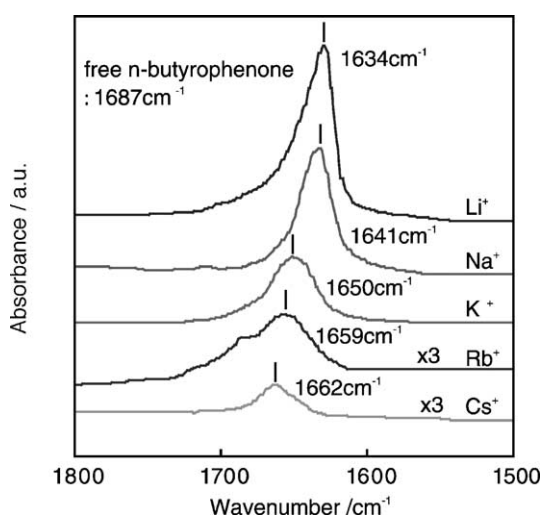


Fig. 1. The IR spectra of *n*-butyrophenone included within alkali metal cation-exchanged ZSM-5 zeolites.

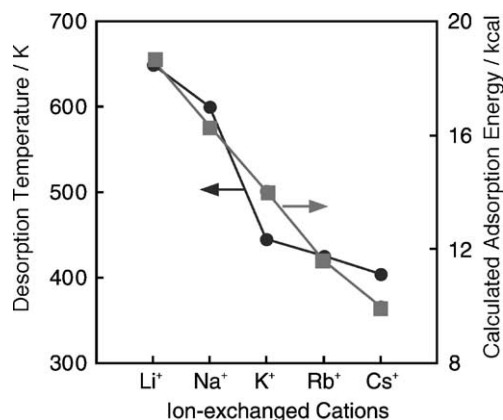


Fig. 2. The effect of the ion-exchanged alkali metal cations on the desorption temperature of *n*-butyrophenone determined by IR measurements and the adsorption energy obtained by the molecular orbital calculations with the supramolecular systems.

cavities. The IR absorption bands assigned to the C=O stretching mode of *n*-butyrophenone can be observed at around 1650 cm^{-1} . The peak at around 1650 cm^{-1} shifts from 1662 to 1634 cm^{-1} by changing the cation from Cs⁺ to Li⁺. Because the peak is sensitively affected by the cations, the peaks at around 1650 cm^{-1} can be assigned to *n*-butyrophenone molecules interacting with the ion-exchanged cations. Changing the cations from Cs⁺ to Li⁺ causes the band to shift to lower wavenumbers and the intensity of the band to stronger. In order to clarify the adsorption state of *n*-butyrophenone molecules, the effect of the ion-exchanged alkali metal cations on the desorption temperature of *n*-butyrophenone included within ZSM-5 has been investigated. The temperatures at which the IR band due to the C=O stretching mode of the adsorbed *n*-butyrophenone disappeared were adapted as the desorption temperatures. The desorption temperatures determined by monitoring the IR peak at around 1650 cm^{-1} , increased when the cations were changed from Cs⁺ to Li⁺ (Fig. 2). These results indicate that with smaller cations, the zeolite cavities have a stronger electrostatic field and the magnitude of the interaction between the cations and *n*-butyrophenone molecules increases with the changing of the cations from Cs⁺ to Li⁺.

n-Butyrophenone included within alkali metal cation-exchanged ZSM-5 exhibits a phosphorescence spectrum at around 420 nm when excited at around 310 nm which can induce the $n\text{--}\pi^*$ transition of carbonyl group. As shown in Fig. 3, *n*-butyrophenone included within the ZSM-5 ion-exchanged with the larger cations, such as Cs⁺, Rb⁺, and K⁺, exhibit vibrational fine structures in the phosphorescence spectra. On the other hand, broad phosphorescence spectra without fine structures are observed on the ZSM-5 ion-exchanged with the smaller cations, such as Na⁺ and Li⁺. Furthermore, as shown in Fig. 4, the relative intensity of the phosphorescence spectra against the amounts of adsorbed *n*-butyrophenone estimated from the

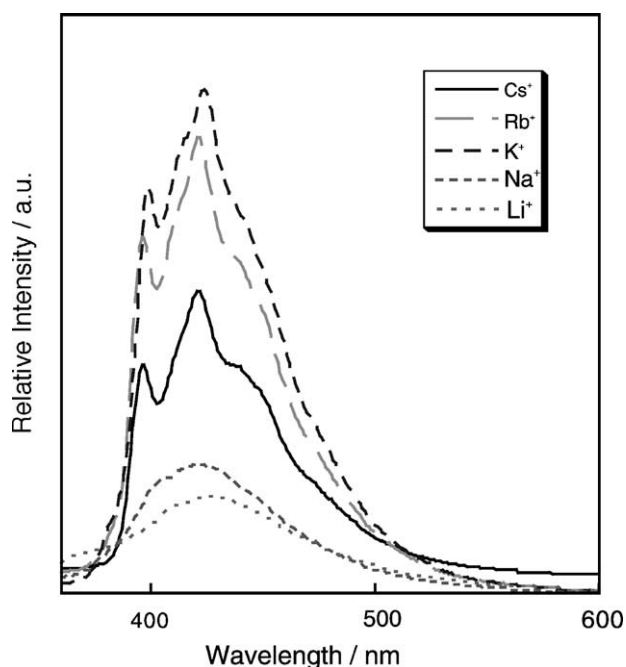


Fig. 3. The phosphorescence spectra of *n*-butyrophenone included within alkali metal cation-exchanged ZSM-5 zeolites (excited at 310 nm).

IR intensity decreases with changing the cation from Cs^+ to Li^+ . The decrease in the relative intensity of the phosphorescence spectra shows the good relationship with the decrease in the photolysis yields observed by changing the cation from Cs^+ to Li^+ . These results also indicate that

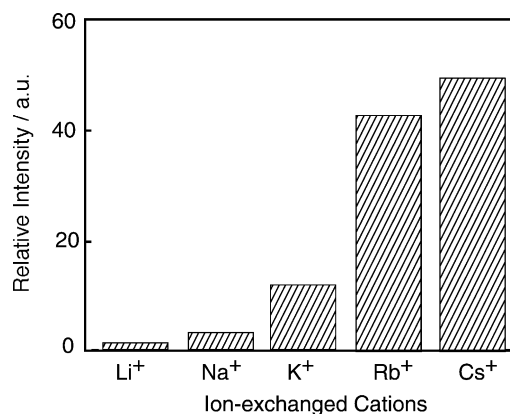


Fig. 4. The relative intensity of phosphorescence spectra against the amounts of adsorbed *n*-butyrophenone estimated from the IR intensity.

with the smaller cations the interaction between the cations and *n*-butyrophenone molecules becomes large enough to depress the photolysis reaction.

3.2. Molecular orbital calculation for the *n*-butyrophenone–zeolite interaction

Fig. 5 shows the model of *n*-butyrophenone molecule in the stable conformation (staggered conformation) directly interacted with the cation-exchanged zeolite framework (ketone- M^+ -frame). Ab initio molecular orbital calculations of such *n*-butyrophenone molecules which directly interact with the cation-exchanged zeolite framework

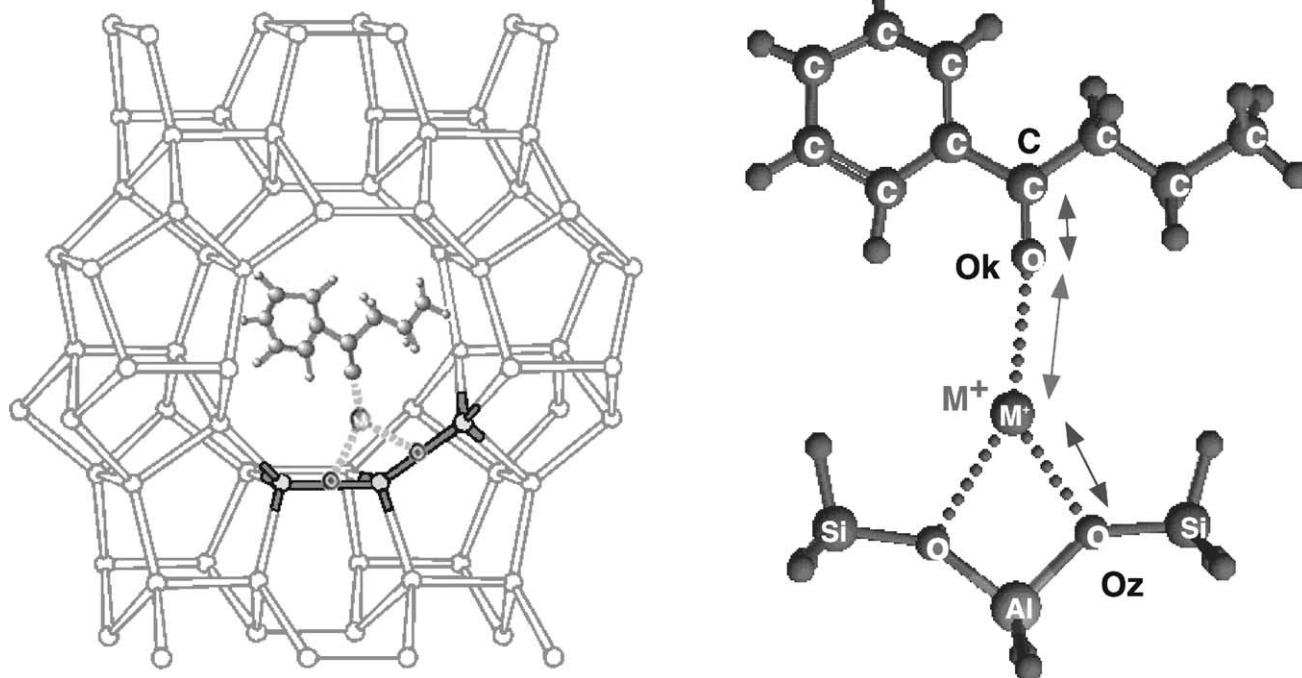


Fig. 5. The model for the system with *n*-butyrophenone adsorbed on alkali metal cation-exchanged zeolite.

Table 2
Bond length (Å) of equilibrium geometries of (*n*-butyrophenone/alkali metal cation/zeolite) systems

Cations	C=O	M ⁺ ...O _z	M ⁺ ...O _k
	bond lengths	bond lengths	bond lengths
Li ⁺	1.209	1.87	1.97
Na ⁺	1.207	2.16	2.24
K ⁺	1.205	2.58	2.68
Rb ⁺	1.204	2.79	2.91
Cs ⁺	1.203	3.00	3.17
Free	1.196		

(ketone-M⁺-frame) provide useful information on the geometry, charge population, heat of adsorption, and vibrational frequencies of the C=O groups of the *n*-butyrophenone molecules. The SCF optimized structures and charge population are summarized in Tables 2 and 3. In the SCF optimized structures of the adsorption of *n*-butyrophenone, the alkali metal cation locates in the configuration which is linear to the C=O bond. The results of ab initio calculations suggest not only that there is no significant overlap between the orbitals of the *n*-butyrophenone molecules and cations but also that they are stabilized on the cations by electrostatic interactions. Although *n*-butyrophenone has the two type of stable conformations (staggered and eclipsed conformations), the obtained values indicated that supramolecular systems with the staggered conformation are more stable than the corresponding system with the eclipsed conformation. As also shown in Tables 2 and 3, the bond length between alkali metal cation and oxygen atom of C=O bond (M⁺...O_k) becomes smaller and C=O bond length becomes longer with the change of cations from Cs⁺ to Li⁺. Also the negative charge of oxygen atom of C=O bond increases indicating that the electrons are localized on oxygen atom of C=O bond. These changes indicate that the interaction between cations and ketones becomes stronger with the change of cations from Cs⁺ to Li⁺.

From the calculated total energy of the supramolecular systems composed of the *n*-butyrophenone molecules in staggered conformations and the cation-exchanged zeolite framework, the interaction energy (adsorption energy) between *n*-butyrophenone and the cation-exchanged zeolite framework (M⁺-frame) is obtained. As shown in Fig. 2, the heat of the adsorption of *n*-butyrophenone calculated with the (ketone-M⁺-frame) systems increases with the changing

Table 3
Total atomic charge of (*n*-butyrophenone/alkali metal cation/zeolite) systems

Cations	M	C	O
Li ⁺	0.550	0.608	-0.642
Na ⁺	0.713	0.596	-0.641
K ⁺	0.811	0.591	-0.636
Rb ⁺	0.839	0.586	-0.628
Cs ⁺	0.862	0.581	-0.619
Free		0.551	-0.546

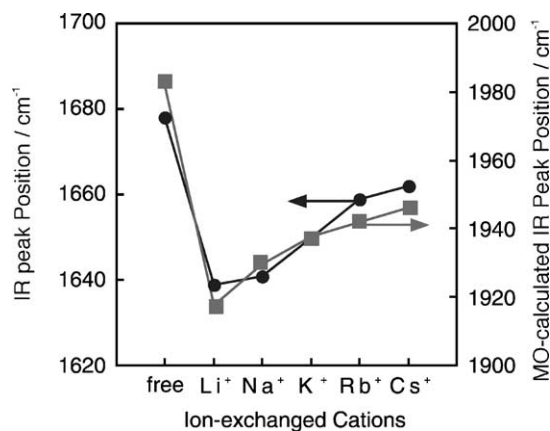


Fig. 6. The comparison between the experimentally observed IR peak positions and the values obtained by the molecular orbital calculations (analysis of the vibrational mode) with the supramolecular systems.

of the cations from Cs⁺ to Li⁺, being in good agreement with the desorption temperature determined from IR measurements. These results also indicate that the interaction between the *n*-butyrophenone and cations becomes stronger when the cations are changed from Cs⁺ to Li⁺.

Fig. 6 shows the effect of the ion-exchanged alkali metal cations on the C=O stretching mode of *n*-butyrophenone determined by experimental IR measurements and molecular orbital calculations. In the analysis of the vibrational mode of the C=O groups, the theoretical harmonic vibrational frequencies of the C=O stretching mode can be seen to shift to the lower values by changing the cations from Cs⁺ to Li⁺, showing a good parallel with the results obtained experimentally by IR measurements. These results support our findings showing not only that the calculation models used for this system in which *n*-butyrophenone molecules interact directly with the cations by an electrostatic interaction is reasonable but also that the magnitude of the interaction increases by changing the cations from Cs⁺ to Li⁺.

4. Conclusions

It can be observed that the efficiency of the photolysis of *n*-butyrophenone included within the alkali metal cation-exchanged zeolites changes with the cation, its extent decreasing by changing the cation from Cs⁺ to Li⁺ in the order of the magnitude of the interaction between the *n*-butyrophenone molecules and the cations. Also, the selectivity for Norrish type I reaction increased by changing the cation from Cs⁺ to Li⁺.

The results obtained both from the experimental measurements and the theoretical calculations indicated that the magnitude of the interaction between the *n*-butyrophenone molecules and the ion-exchanged cations increased by changing the cation from Cs⁺ to Li⁺. As shown in reaction Scheme 1, the Norrish type II reaction proceeds through the formation of a 1,4-biradical intermediate. A favorable

conformation, i.e., a six-membered intermediate, is required for a γ -hydrogen atom abstraction to take place. In the strong interaction between the *n*-butyrophenone molecules and cations within the zeolite cavities, the formation of such a six-membered transition state is considerably suppressed, its extent strongly depending on the kind of metal cation. The stronger interaction between the *n*-butyrophenone molecules and the smaller cations led to the decrease in the efficiency of the photolysis of *n*-butyrophenone, while the strong interaction is comparatively preferable for the Norrish type I reaction.

Acknowledgements

This work has been supported by the Grant-in-Aid Scientific Research from the Ministry of Education, Science, Culture, and Sports of Japan (Grants 12042271 and 13650845).

References

- [1] M. Anpo, T. Matsuura (Eds.), *Photochemistry on Solid Surfaces*, Elsevier, Amsterdam, 1989.
- [2] J.K. Thomas, *Chem. Rev.* 93 (1993) 301.
- [3] M. Anpo (Ed.), *Photofunctional Zeolites*, Nova Sci. Pub. Inc., New York, 2000.
- [4] H. Nishiguchi, M. Anpo, *J. Photochem. Photobiol. A* 77 (1994) 183.
- [5] H. Nishiguchi, K. Yukawa, H. Yamashita, M. Anpo, *Res. Chem. Intermed.* 21 (1995) 885.
- [6] H. Nishiguchi, K. Yukawa, H. Yamashita, M. Anpo, *J. Photochem. Photobiol. A* 99 (1995) 1.
- [7] H. Nishiguchi, S. Okamoto, M. Nishimura, H. Yamashita, M. Anpo, *Res. Chem. Intermed.* 24 (1998) 849.
- [8] H. Yamashita, M. Anpo, in: M. Anpo (Ed.), *Photofunctional Zeolites*, Nova Sci. Pub. Inc., New York, 2000, pp. 99–127.
- [9] H. Yamashita, N. Sato, M. Anpo, T. Nakajima, M. Hada, H. Nakatsuji, *Stud. Surf. Sci. Catal.* 105 (1997) 1141.
- [10] H. Yamashita, A. Tanaka, M. Nishimura, M. Anpo, *Stud. Surf. Sci. Catal.* 117 (1998) 651.
- [11] H. Yamashita, M. Nishimura, H. Bessho, S. Takada, T. Nakajima, M. Hada, H. Nakatsuji, M. Anpo, *Res. Chem. Intermed.* 27 (2001) 89.
- [12] N.J. Turro, *Pure Appl. Chem.* 58 (1986) 1219.
- [13] V. Ramamurthy, *Photochemistry in Organized and Constrained Media*, VCH, New York, 1991.
- [14] V. Ramamurthy, D.F. Eaton, J.V. Caspar, *Acc. Chem. Res.* 25 (1992) 299.
- [15] V. Ramamurthy, D.R. Corbin, L.J. Johnston, *J. Am. Chem. Soc.* 114 (1992) 3870.
- [16] V. Ramamurthy, J.V. Caspar, D.F. Eaton, E.W. Kuo, D.R. Corbin, *J. Am. Chem. Soc.* 114 (1992) 3882.
- [17] A. Redondo, P.J. Hay, *J. Phys. Chem.* 97 (1993) 11754.
- [18] H. van Koningsveld, H. van Bekkum, J.C. Jansen, *Acta Crystallogr. B* 43 (1987) 127.
- [19] H. van Koningsveld, H. van Bekkum, J.C. Jansen, *Zeolites* 10 (1990) 235.
- [20] F.S. Wettack, W. Albert Noyes Jr., *J. Am. Chem. Soc.* 90 (1968) 3901.
- [21] H.E. O'Neal, R.G. Miller, F. Gunderson, *J. Am. Chem. Soc.* 96 (1974) 3351.